Proceedings of the
9th Graz Brain-Computer Interface Conference 2024
10.3217/978-3-99161-014-4-035

SPATIAL AND SPECTRAL CHANGES IN CORTICAL POTENTIALS DURING PINCHING VERSUS THUMB AND INDEX FINGER FLEXION

Panagiotis Kerezoudis[1,2]; Michael A Jensen[1,3]; Harvey Huang[3], Jeffrey G. Ojemann[4]; Bryan T. Klassen[5], Nuri F. Ince[2,6]; Dora Hermes[6]; Kai J Miller[2,6]

[1]Division of Neuroscience, Mayo Graduate School of Biomedical Sciences, Rochester, MN, USA
[2]Department of Neurologic Surgery, Mayo Clinic, Rochester, MN, USA
[3]Medical Scientist Training Program, Mayo Clinic, Rochester, MN, USA
[4]Department of Neurosurgery, Seattle Children's Hospital, Seattle, Washington
[5]Department of Neurology, Mayo Clinic, Rochester, MN, USA
[6]Department of Physiology and Biomedical Engineering, Mayo Clinic, Rochester, MN, USA.

E-mail: kerezoudis.panagiotis@mayo.edu

ABSTRACT: We analyzed the electrocorticographic signals of 3 patients implanted with subdural electrode arrays for identification of seizure foci. Patients performed screen cue-based flexion movement of the thumb or index finger, or a pinch movement of both. Broadband power changes with each movement were estimated. Topological maps for each type of movement were created using co-registered brain renderings, and the overlap in spatial extent was quantified using a resampling metric. Activation during pinching was compared with thumb flex, index flex and three composite metrics: the maximum, the geometric mean and a modified geometric mean. Significant increase in broadband power was observed in all three patients when pinch (max signed r^2 0.64-0.80-0.89), thumb flexion (0.63-0.72-0.89) or index flexion (0.66-0.67-0.83) was performed compared to rest. Spatial overlap was highest between pinching and index flexion (69-87%, all $p < .001$), followed by the modified geometric mean (61-96%, all $p < .001$), while thumb flexion had the lowest overlap of all analyzed metrics (27-77%, significant in 2/3).

INTRODUCTION

The hallmark of human motor behavior is the ability to perform fine individual finger movements. Dexterous hand gestures are essential to carrying out activities of daily living and can be considered as a combination of individual finger movements with varying degrees of freedom, particularly flexion and extension. Interestingly, certain moves, including reaching, grasping (palmar or pincer), transporting, and placing have been previously proposed as motor primitives that represent building blocks to execute an overall goal-directed action, such as a monkey reaching for a seed, grasping it, bringing it towards the mouth and finally eating it [1].

Whether the neural representation of composite moves is equal to the linear summation of their constituents (e.g. palmar grasp vs concurrent all-finger flexion) or non-linear and therefore, not easily predictable, remains unknown and it is an area of ongoing electrophysiology and imaging research [2,3]. Recordings of the human brain cortical surface the last 30-40 years have revealed movement-related signals over the motor and sensory regions with high accuracy [4–7]. Specifically, electrocorticography (ECoG) experiments have demonstrated that hand and tongue movement are associated with spatially focal but spectrally broadband changes in the frontoparietal cortex [6,8]. Distinct individual finger movements have been identified with electrode spacing resolution as low as 1cm using subdural recordings [9].

The spectral and spatial relationship between individual finger movement and synergistic action has not yet been fully elucidated, and the extent to which grasping movements represent sums of the individual finger moves or activate different brain areas, e.g. premotor cortex, (posterior) parietal cortex etc. Herein, we report our findings in 3 young patients with medically refractory epilepsy that underwent invasive ECoG recordings as part of their seizure workup. We demonstrate the spatially focal spectral changes that occur with thumb flexion, index flexion and pinching and compare these three movement types in their spatial overlap.

MATERIALS AND METHODS

Ethics statement: All patients participated in a purely voluntary manner and provided informed consent, based on protocols approved by the Institutional Review Board of the University of Washington, Seattle.

Patient population: We recruited 3 patients (2 females, aged 18, 21 and 19 years) that underwent invasive clinical EEG monitoring for localization of seizure foci as part of their workup for medically refractory epilepsy using subdural ECoG grids.

Published by
Verlag der Technischen Universität Graz

10.3217/978-3-99161-014-4-035

Electrical recordings: The platinum ECoG arrays were configured as a combination of grid (8x8 or 4x8) arrays and strip arrays, numbering a total of 32 to 81 contacts (i.e. channels). The diameter of the electrode contacts was 4mm and the inter-electrode distance was 10mm. These arrays were surgically placed by one of the senior authors (J.G.O). The ECoG signals were split into two identical sets, one towards the clinical EEG system (XLTEK, Oakville, Ontario, Canada) and the research set was recorded using the Synamps2 (Neuroscan, El Paso, TX) biosignal amplifiers at 1 kHz with a bandpass-filter at 0.3-200 Hz. Finger position was recorded using a sensor dataglove (5DT, Irvine, CA). The general purpose BCI2000 software was used for stimulus presentation and ECoG signal data collection [10].

*Cortical rendering and electrode localization: T*he cortical surface from a preoperative MRI was rendered using either Freesurfer or Spm5 software in order to determine the relationship between the gyral anatomy and electrode position. The electrode positions were calculated after co-registering the post-operative computed tomography (CT) to the pre-operative MRI using the CTMR package by Hermes et al., 2010, which has been shown to accurately localize the electrode positions within a ~4mm error [11].

Movement tasks: Subjects were presented with a word cue displayed on a bedside monitor to perform the following self-paced movement tasks, each on a separate run: 1) pinching move between the thumb and the index finger or 2) individual thumb or index finger flexion. A 2-second rest trial (blank screen) followed each movement trial. There were up to 30 cues for each movement type. Segmentation of movement vs rest period was performed based on visual inspection of the data glove trace and marking the initiation and termination of movement. A total of 10-15 movement/rest trials were completed for each task.

Signal pre-processing: The potential measured at each electrode was re-referenced with respect to the common average of all electrodes. Electrodes significant for artifact or epileptiform activity were visually inspected, removed from re-referencing and omitted prior to further analysis.

Power spectral snapshots: Power spectral snapshots using Welch's method and a Hann window of 1s were generated for the entire experiment in each electrode as well as separately for movement and rest blocks. In addition, we mean-normalized the log power spectra by dividing the power spectrum for each trial with the mean electrode power spectrum. The frequency range of interest included 1-200 Hz.

Dynamic power spectrum: We generated time-frequency approximations after convolving the voltage time-series data with a Morlet wavelet (10 cycles) in order to estimate the amplitude and phase of the signal across the frequency range for every point in time.

Power spectrum decoupling: We performed decoupling of the power spectra using a previously established method by Miller et al, 2009 [12]. In summary, we performed Principal Component Analysis (i.e. eigendecomposition) of the power spectral density-covariance matrices (freq [*f*], chan [*k*], trials [*q*]). The resultant eigenvectors (principal spectral components-PSCs) reveal which frequencies vary in power together and are ordered according to the value of the corresponding eigenvalue. It has been shown that the 1st PSC corresponds to broadband spectra (i.e. spanning all frequency ranges), whereas the 2nd-4th PSCs typically capture rhythmic power spectral phenomena (i.e. mu rhythm, alpha rhythm etc). In addition, the projection of the dynamic spectrum onto the 1st PSC will yield the logarithm of the time course of the power spectrum power law coefficient $P(f, t) = A(t)*f^{-\chi}$ [13]. This logarithm was subsequently smoothed with a Gaussian window (250 ms), z-scored and re-exponentiated in order to obtain the broadband trace plotted in Fig. 1. This broadband power time course has been shown to be a robust estimate of behaviorally relevant local cortical activity as well as predictive of the finger movement time course, as measured by the data glove [5]. Finally, we calculated the signed r^2 cross-correlation values from broadband activity, between each movement modality (pinching, thumb flexion, or finger flexion) and rest. Movement trials were compared with the rest trials that followed the same movement type [14]. Thus, r^2 represents the percentage in variance in the joint distribution of movement-rest blocks, that can be explained by a difference in the movement and rest trial means, respectively.

$$r^2 = \frac{(\bar{m} - \bar{r})^3}{|\bar{m} - \bar{r}|^* \sigma^2_{mUr}} \frac{N_m * N_r}{N^2_{mUr}}$$

Quantifying spatial overlap: The spatial extent of overlap and degree of change in broadband power activity was quantified and compared using a resampling metric. In summary, for measures of type X_n and Y_n (n denoting the electrode), the true overlap (O^T_{XY}) was calculated from the pairwise dot product of the broadband r^2 value. The spatial overlap metric was calculated by dividing the true overlap with the maximum possible overlap (O^M_{XY}), by computing the dot product of distributions X_n and Y_n assorted in ascending order. The electrodes were subsequently scrambled 10^6 times (n→m) and a surrogate overlap was obtained from each permutation (O^S_{XY}). Finally, p-value for statistical significance was estimated as the percentage of surrogate distributions O^S_{XY} that were greater than O^T_{XY} (or the percentage that were less in case $O^T_{XY}<0$). The methodology is graphically displayed in Fig. 2. The r^2 electrode activation maps of the following conditions were compared with pinching [summarized in Table 1]: finger flexion, thumb flexion, their maximum value per channel, their geometric mean and modified geometric mean.

Published by
Verlag der Technischen Universität Graz

10.3217/978-3-99161-014-4-035

Table 1. Summary of metrics used for the analysis of spatial overlap with pinching.

Condition	Rationale
Thumb flexion r^2_{thb}	Constituents of pinching movement.
Index flexion r^2_{idx}	
Maximum value of thumb flex, index flex $\max\{r^2_{thb}, r^2_{idx}\}$	Activation reflects the maximal activity evoked by each individual finger movement (i.e. the union of two activation sets).
Geometric mean of thumb flex and index flex $\sqrt{\lvert r^2_{thb} * r^2_{idx} \rvert}$	Activation reflects the average activity evoked by each individual finger movement (i.e. the intersection of two activation sets).
Modified geometric mean of thumb flex and index flex $1-\sqrt{\lvert (1-r^2_{thb})*(1-r^2_{idx}) \rvert}$	Activation reflects the average activity evoked by each individual finger movement (i.e. the complement of the intersection of the non-activation sets).

RESULTS

Spectral changes related to movement: Across all 3 subjects, we observed significant increase in broadband power in the higher frequencies with movement and decrease in power in narrowband, lower-frequency oscillations (Fig. 1). Specifically, the maximum channel r^2 values associated with movement were 0.63/0.72/0.89 for thumb flexion, 0.66/0.67/0.83 for index finger flexion and 0.64/0.80/0.89 for pinching. Broadband power increases following each movement type were more spatially focused, whereas motor beta rhythm (12-20 Hz) power decrease was more widely distributed over the cortical surface. Following decoupling of the power spectrum as described above, we projected the dynamic spectrum to the first eigenvector and recreated the log(broadband) timeseries. Following smoothing with a Gaussian window, z-scoring and re-exponentiation, we found that the time course of broadband activation matched finger movement with high accuracy.

Somatotopy of movement-related spectral changes: The r^2 activation values corresponding to each channel in the subdural grid were plotted on the 3D brain renderings for each individual finger movement type as well as their composite metrics (Fig. 3). In all three patients, spatial overlap between pinch and index flexion (69-87%, all $p<.001$) was considerably higher compared to pinch and thumb flexion (27-77%; significant in 2/3 patients). Furthermore, the modified geometric mean metric performed similarly or better compared to the index flex (61-96%), while the max (39-89%) and geometric mean (68-81%) metrics ranked in between.

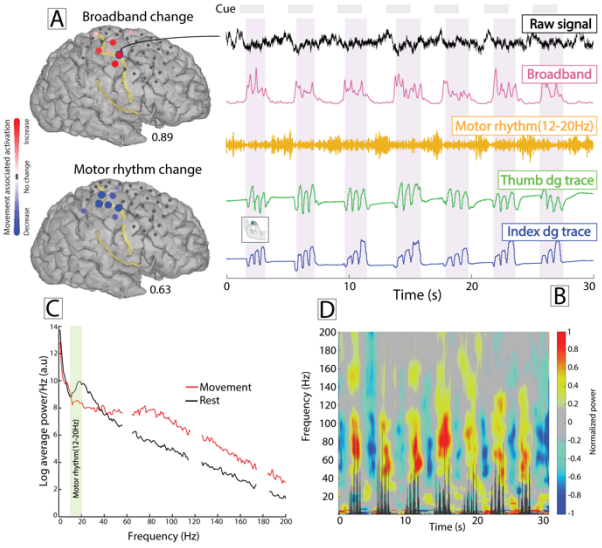

Figure 1. Electrocorticographic (ECoG) activity in the right frontoparietal cortex during pinch movement and rest (subject 3). (A) Topological maps demonstrating focal broadband power increase and more widespread spatial distribution in motor rhythm (12-20 Hz) power decrease. (B) Spectral changes demonstrate excellent correlation with finger movement. (C) Power spectral density plot from the entire behavioral task showing decrease in low-frequency oscillations and broadband increase across the rest of the frequency range, during movement (red) compared to rest (black). (D) Time-varying power spectral density plot during the same period of recording. The black trace inset represents the 1st derivative of thumb movement.

DISCUSSION

In the present study, we analyzed the cortical activity in three patients implanted with subdural electrode arrays during three types of finger movement, i.e. thumb flexion, index flexion and pinching, and compared their spatial overlap in broadband activation. Overall, we observed the spatial overlap between pinching and index flexion to be significantly higher compared to thumb flexion, reflecting a considerably smaller digit movement of the latter during the combined motor behavior. This aligns with the results by Cramer et al., who demonstrated that the degree of muscle activation, such as force of squeezing, correlates with the volume of activated cortical tissue as measured by fMRI bold signal [15].

Published by
Verlag der Technischen Universität Graz

10.3217/978-3-99161-014-4-035

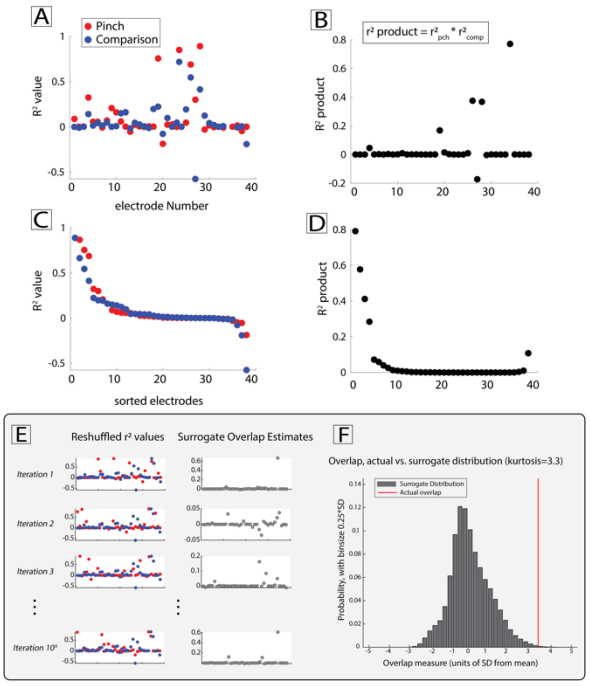

Figure 2. Demonstration of the method for quantifying the overlap in spatial distribution. (A) The r^2 value, as a metric of activation during movement vs rest, is computed and plotted for each electrode, during pinching versus thumb flexion, index flexion or one of the other metrics we used (collectively labeled here as 'comparison'). (B) The overlap can be quantified as the dot product across electrodes, thereby denoting that activities are paired together at each electrode. (C) We can probe all of the possible configurations of activation values by reshuffling the electrode positions (left panels) for one of the conditions (pinch) and recalculating the dot products (right panels). This is done 10^6 times, generating the distribution of surrogate dot products. (D) The generated surrogate distribution can be used to estimate a p-value for the significance of the overlap.

To date, the majority of work investigating neuronal representation of multi-task computations is derived from simulated models, non-human primate recordings or human fMRI experiments [16,17]. Evarts' pioneering work demonstrated linear relation of single-unit neuronal activity with forces and torques about the wrist [18]. Later studies refuted this notion, supporting altered gain of this relation depending on the size of inertial load and the anticipated range of force.[19,20] For example, Shah et al. recently reported their findings from recorded motor activity from high-density cortical arrays in two patients with tetraplegia that performed single, pairwise and higher order finger movements [2]. Given the subjects' medical history, kinematics was captured and analyzed using an animated hand (Unity Software, Unity Technologies, San Francisco). They observed that neural activity associated with multiple finger movements aligned with a 'pseudo-linear' summation of individual finger activities, i.e. had lower magnitude, which authors attributed to vector unit-normalization.

Chestek et al. classified different hand posture ECoG signals with subdural micro- and macro-electrodes implanted over the primary sensorimotor areas [21]. The authors examined 4 finger movements and 4 distinct isometric hand postures (pinch, fist, splay and point). Similar to our findings, they observed significant co-modulation of the thumb electrode (up to 93% likelihood) for index, and observed index finger flexion and pinching to be similar movements that could be decoded at 79% correct based on 'gamma-band' power (66-114Hz) [21]. Our study build further upon that work by delving into the topological representation of composite vs individual finger movements.

Recent work in monkeys has revealed similar findings. Naufel et al. investigated the relation between primary motor cortex (M1) and muscle activity (as captured by electromyography, EMG) during three wrist movement tasks of varying dynamical load and forces [3]. The authors observed that a greater proportion of EMG changes were explained by a linear model of M1 activity supplemented by a condition-dependent gain. In our analysis, the non-linear metric of modified geometric mean explained a greater proportion of spatial overlap compared to maximum value and geometric mean. Nonetheless, the association between biological underpinnings of more complex limb movements and nonlinear dynamics remains to be determined; potential explanatory phenomena may include modulation of cortical activity (M1, premotor etc) by subcortical structures and differential inhibitory interneuron activity.

Implications for future research: These findings have implications for brain-computer interface applications. One common limitation of motor-controlled brain-computer interface (BCI) in non-human primates is the suboptimal coupling between neural activity and movement output [22]. Subsequent iterations of cortically-based BCI designs should take into consideration the strength and the spatiotemporal patterns of neural signals and how these relate to muscular activity. Future research can further expand on our work to investigate how individual finger actions relate to and overlap with other complex gestures, such as palmar grasping, squeezing and pointing.

Limitations: First, our sample consisted only of 3 subjects. Second, we employed standard-scale clinical ECoG, rather than high-density research grids; the latter have been shown to have superior spatial performance in 6 elementary movements in the alpha, beta and gamma frequency bands [21]. Third, we were unable to incorporate kinetics and/or kinematics in our analysis to correlate with the ECoG signal. The data glove captures mean deformation of an electrically conductive elastomer with piezoresistive properties but does not allow for detailed analysis of force of contraction or degree of displacement/range of motion in the interphalangeal joints.

Published by
Verlag der Technischen Universität Graz

10.3217/978-3-99161-014-4-035

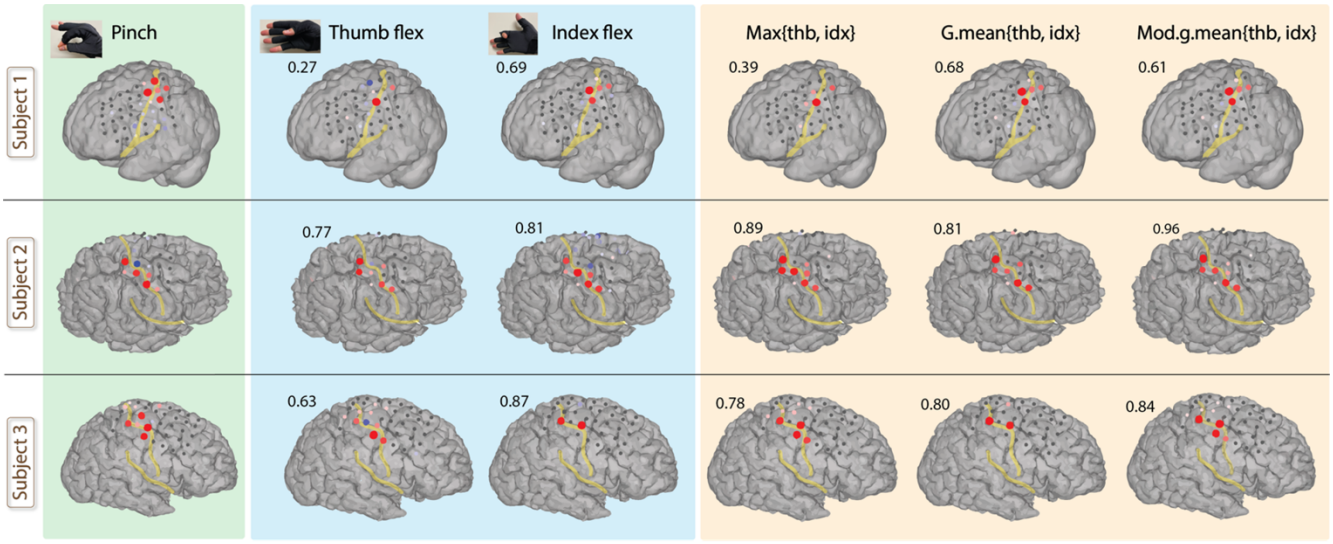

Figure 3. Topological maps in each subject demonstrating changes in broadband power at different cortical sites for pinching (green panel), thumb and index finger flexion (blue panel) and three combined r^2 metrics (orange panel): the maximum, the geometric mean and the modified geometric mean; please refer to Methods for detailed description. The spatial overlap of each condition with pinching is shown on the top left corner of the brain renderings. Overall, it can be appreciated that index flexion, followed by the modified geometric mean, had the highest overlap with pinching.

CONCLUSION

For pinch, the ECoG signal seems to comprise a combination of the signals from the individual thumb and index movements, with considerably larger overlap with the latter. This analysis may provide insight into the tuning of the motor cortex toward specific types of motor behaviors and help refine currently available BCI control algorithms and their therapeutic efficacy.

ACKNOWLEDGEMENTS

All patients participated in a purely voluntary manner, after providing informed written consent, under experimental protocols approved by the Institutional Review Board of the University of Washington (#12193). All patient data was anonymized according to IRB protocol, in accordance with HIPAA mandate. It was made available through the library described in “A Library of Human Electrocorticographic Data and Analyses” by Kai Miller [*Miller, Kai J. "A library of human electrocorticographic data and analyses." Nature human behaviour 3.11 (2019): 1225-1235*]. This work was also supported by the National Institutes of Health (NIH) NINDS U01-NS1286.

REFERENCES

[1] Hemeren PE, Thill S. Deriving motor primitives through action segmentation. Front Psychol. 2010;1:243.

[2] Shah NP, Avansino D, Kamdar F, Nicolas C, Kapitonava A, Vargas-Irwin C, et al. Pseudo-linear Summation explains Neural Geometry of Multi-finger Movements in Human Premotor Cortex. bioRxiv [Internet]. 2023 Oct 12; Available from: http://dx.doi.org/10.1101/2023.10.11.561982

[3] Naufel S, Glaser JI, Kording KP, Perreault EJ, Miller LE. A muscle-activity-dependent gain between motor cortex and EMG. J Neurophysiol. 2019 Jan 1;121(1):61–73.

[4] Crone NE, Miglioretti DL, Gordon B, Sieracki JM, Wilson MT, Uematsu S, et al. Functional mapping of human sensorimotor cortex with electrocorticographic spectral analysis. I. Alpha and beta event-related desynchronization. Brain. 1998 Dec;121 (Pt 12):2271–99.

[5] Miller KJ, Hermes D, Honey CJ, Hebb AO, Ramsey NF, Knight RT, et al. Human motor cortical activity is selectively phase-entrained on underlying rhythms. PLoS Comput Biol. 2012 Sep 6;8(9):e1002655.

[6] Miller KJ, Honey CJ, Hermes D, Rao RPN, denNijs M, Ojemann JG. Broadband changes in the cortical surface potential track activation of functionally diverse neuronal populations. Neuroimage. 2014 Jan 15;85 Pt 2:711–20.

[7] Crone NE, Miglioretti DL, Gordon B, Lesser RP. Functional mapping of human sensorimotor cortex with electrocorticographic spectral analysis. II. Event-related synchronization in the gamma band. Brain. 1998 Dec;121 (Pt 12):2301–15.

[8] Miller KJ, Leuthardt EC, Schalk G, Rao RPN, Anderson NR, Moran DW, et al. Spectral changes in cortical surface potentials during motor movement. J Neurosci. 2007 Feb 28;27(9):2424–32.

[9] Schalk G, Miller KJ, Anderson NR, Wilson JA, Smyth MD, Ojemann JG, et al. Two-dimensional movement control using electrocorticographic signals in humans. J Neural Eng. 2008 Mar;5(1):75–84.

[10] Schalk G, McFarland DJ, Hinterberger T, Birbaumer N, Wolpaw JR. BCI2000: a general-

Published by
Verlag der Technischen Universität Graz

10.3217/978-3-99161-014-4-035

purpose brain-computer interface (BCI) system. IEEE Trans Biomed Eng. 2004 Jun;51(6):1034–43.
[11] Hermes D, Miller KJ, Noordmans HJ, Vansteensel MJ, Ramsey NF. Automated electrocorticographic electrode localization on individually rendered brain surfaces. J Neurosci Methods. 2010 Jan 15;185(2):293–8.
[12] Miller KJ, Zanos S, Fetz EE, den Nijs M, Ojemann JG. Decoupling the cortical power spectrum reveals real-time representation of individual finger movements in humans. J Neurosci. 2009 Mar 11;29(10):3132–7.
[13] Miller KJ, Sorensen LB, Ojemann JG, den Nijs M. Power-law scaling in the brain surface electric potential. PLoS Comput Biol. 2009 Dec;5(12):e1000609.
[14] Jensen MA, Huang H, Valencia GO, Klassen BT, van den Boom MA, Kaufmann TJ, et al. A motor association area in the depths of the central sulcus. Nat Neurosci. 2023 Jul;26(7):1165–9.
[15] Cramer SC, Weisskoff RM, Schaechter JD, Nelles G, Foley M, Finklestein SP, et al. Motor cortex activation is related to force of squeezing. Hum Brain Mapp. 2002 Aug;16(4):197–205.
[16] Driscoll L, Shenoy K, Sussillo D. Flexible multitask computation in recurrent networks utilizes shared dynamical motifs [Internet]. bioRxiv. 2022 [cited 2024 Jan 15]. p. 2022.08.15.503870. Available from: https://www.biorxiv.org/content/10.1101/2022.08.15.503870
[17] Ito T, Murray JD. Multitask representations in the human cortex transform along a sensory-to-motor hierarchy. Nat Neurosci. 2023 Feb;26(2):306–15.
[18] Evarts EV. Relation of pyramidal tract activity to force exerted during voluntary movement. J Neurophysiol. 1968 Jan;31(1):14–27.
[19] Humphrey DR. Relating motor cortex spike trains to measures of motor performance. Brain Res. 1972 May 12;40(1):7–18.
[20] Hepp-Reymond M, Kirkpatrick-Tanner M, Gabernet L, Qi HX, Weber B. Context-dependent force coding in motor and premotor cortical areas. Exp Brain Res. 1999 Sep;128(1-2):123–33.
[21] Chestek CA, Gilja V, Blabe CH, Foster BL, Shenoy KV, Parvizi J, et al. Hand posture classification using electrocorticography signals in the gamma band over human sensorimotor brain areas. J Neural Eng. 2013 Apr;10(2):026002.
[22] Kuo CH, Blakely TM, Wander JD, Sarma D, Wu J, Casimo K, et al. Context-dependent relationship in high-resolution micro-ECoG studies during finger movements. J Neurosurg. 2019 Apr 26;132(5):1358–66.

Published by
Verlag der Technischen Universität Graz